

**Characterization of Dihydropteridine Reductase using Spectroscopic Techniques:  
Determining the Mechanisms Governing the Enzyme's Activity by Monitoring its  
Interactions with its Ligand, Trimethoprim**

Honors Thesis  
Prepared by Vanessa Crevecoeur  
Dr. Ruel Desamero, Mentor

*Chemistry/ Natural Sciences Department  
York College, City University of New York*

May 2007

**Table of Contents**

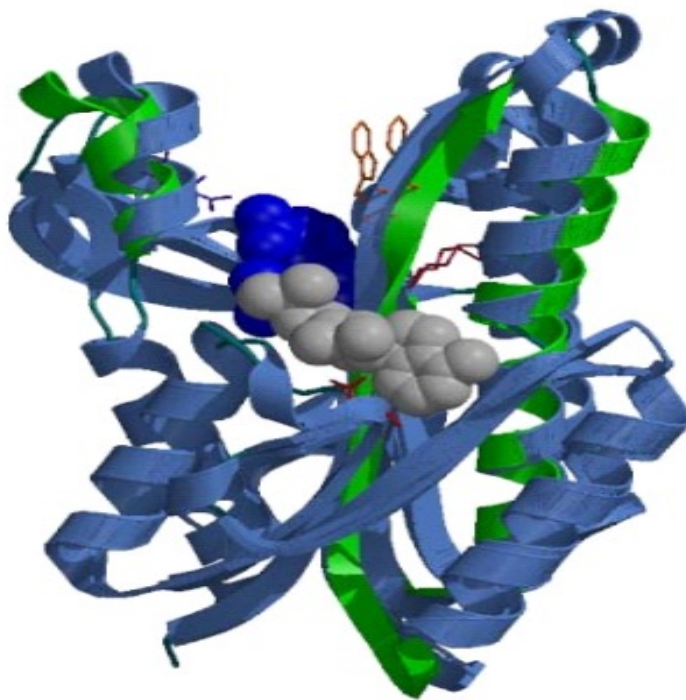
<i>Abstract</i> .....	3
I. Introduction .....	4
II. Protein Extraction and Enzymatic Assay .....	9
III. Methods and Instrumentation .....	14
1. Ultraviolet- Visible Spectroscopy .....	14
2. Fluorescence Spectroscopy .....	15
3. Fourier- Transform Infrared Spectroscopy .....	17
4. <i>Ab initio</i> Calculations .....	18
IV. Results .....	19
1. UV- Vis and Fluorescence Spectroscopy .....	19
2. Infrared Spectroscopy and Calculations- generated .....	22
V. Discussion and Conclusion .....	29
Acknowledgements .....	32
<i>References</i> .....	33

### Abstract

The enzyme Dihydropteridine reductase (DHPR) is found in the brain where it participates in the reproduction of tetrahydrobiopterin from quinonoid-dihydrobiopterin during the hydroxylation cycle of phenylalanine, tyrosine and tryptophan. In this synthesis, tetrahydrobiopterin is a cofactor to the phenylalanine, tyrosine and tryptophan hydroxylases. This hydroxylation process generates the precursors of important neurotransmitters such as L-Dopa, catecholamine and serotonin. In recent researches, the X-ray crystal structure of the apoenzyme and the cofactor bound enzyme was determined. However, the crystal structure of the enzyme together with its substrate and cofactor are yet to be known. Also, a mechanism has been proposed to illustrate the interactions happening between the enzyme and its substrate, dihydrobiopterin. Thus, using spectroscopic techniques, we are probing the interactions between the enzyme, its cofactor, NADH, and its ligand, TMP, both in binary and ternary complexes. TMP shares similar structural features with dihydrobiopterin, which makes it a suitable inhibitor of the enzyme. So far, data obtained from fluorescence measurement suggest interactions between the enzyme and its ligand. Infrared spectroscopy and *Ab initio* calculations are used to identify the specific nature of those interactions.

## I. Introduction

Dihydropteridine Reductase is a protein constituted of two identical subunits. Previous studies have developed the X-Ray crystal structure of the enzyme as it is bound to its cofactor, NADH. Varughese (1992), Su (1993) and their coworkers also characterize DHPR as a  $\alpha/\beta$  protein with a Rossmann- type dinucleotide fold allowing for the NADH binding. They also find out that the dimerization of the protein is facilitated by a four- helix motif (Su et al., 1993; Varughese et al., 1992). In addition, it is observed, from determining the crystal structure of the apoenzyme, that NADH is required to enhance the stability of the enzyme and for the availability of the active site (Su et al., 1993, 1994; Varughese et al., 1992).

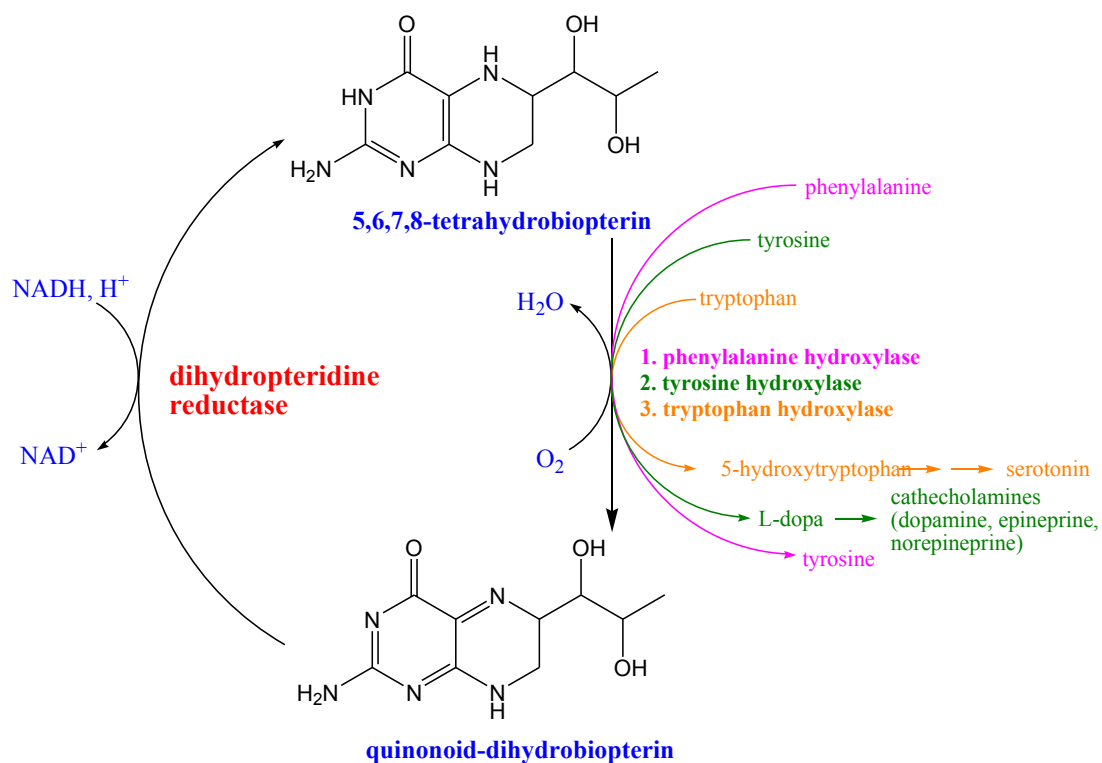


**Scheme 1 X-ray crystal structure of the protein bound to its cofactor NADH.**

Scheme 1 shows the crystal structure of the protein when it is bound to the cofactor 1,4-dihyronicotinamide adenine dinucleotide (NADH). The cofactor is in CPK structure in the

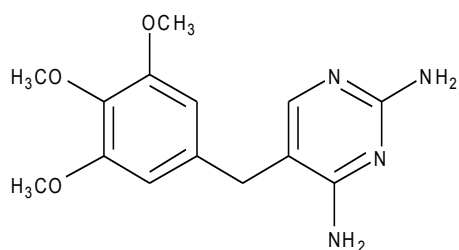
center of the protein molecule. The blue structure corresponds to that of the *apo* form of the enzyme. The green structure represents the enzyme's domains that move upon binding of the cofactor. In the enzyme's structure, there is a tryptophan ring that is opposite the adenine of the NADH. It has been suggested that when a ligand, such as trimethoprim, is present, it would fit between those two sets of rings. If it is the case, anytime we would excite the enzyme, there will be a noticeable transfer of energy between the enzyme and its substrate (Su et al., 1993; Varughese et al., 1992).

The enzyme DHPR participates in the hydroxylation cycle of phenylalanine, tyrosine and tryptophan in the brain (Scheme 2). Those three amino- acids are known as Large Neutral Amino-Acids (LNAAs). The LNAAs are important for development, particularly for brain development and proper functioning (Koch, 2001, as cited in Schuet, 2001). Essentially, DHPR recycles tetrahydrobiopterin from quinonoid- dihydrobiopterin. This step is of major importance since the hydroxylases involved in the process are all tetrahydrobiopterin- dependent. Thus, a deficiency of DHPR would result in a reduced production of tetrahydrobiopterin that could lead to an accumulation of the amino- acids in the blood. As phenylalanine accumulates in the bloodstream, neurological conditions, such as Phenylketonuria, could develop. In 1975, Kaufman and colleagues identified the first DHPR- deficiency related case of Phenylketonuria (Kaufman et al., 1975). Basically, the body of a phenylketonuric lacks the ability to metabolize effectively the phenylalanine, which will then be in excess in the bloodstream. This condition will ultimately cause mental retardation (Nylan, 1984). Therefore, it becomes important to understand the mechanisms governing DHPR's activity in order to devise efficient regulatory techniques that could remedy or prevent the enzyme's deficiency.

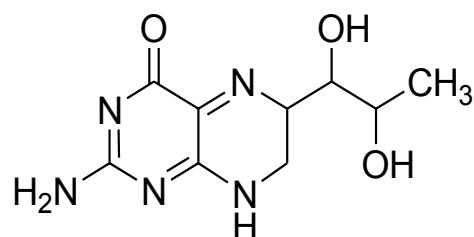


**Scheme 2 Hydroxylation process of amino acids in the brain, pertaining to the biological relevance of DHPR.**

To probe the potential interactions between the enzyme and its substrate, quinonoid-dihydrobiopterin, we will study how the enzyme interacts with one of its inhibitors, trimethoprim. Recent studies have shown that trimethoprim share similar structural features with quinonoid-dihydrobiopterin, which makes it suitable for our study.

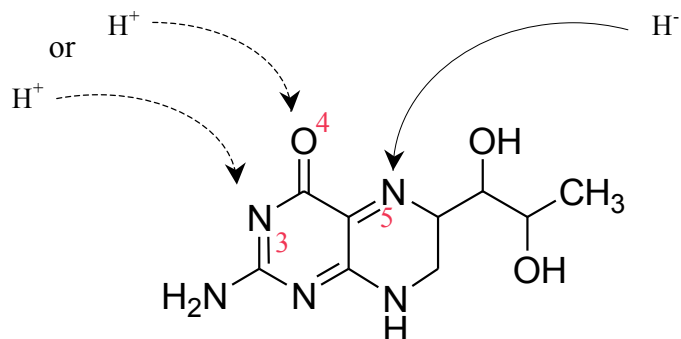


**Scheme 3 Trimethoprim (TMP)**



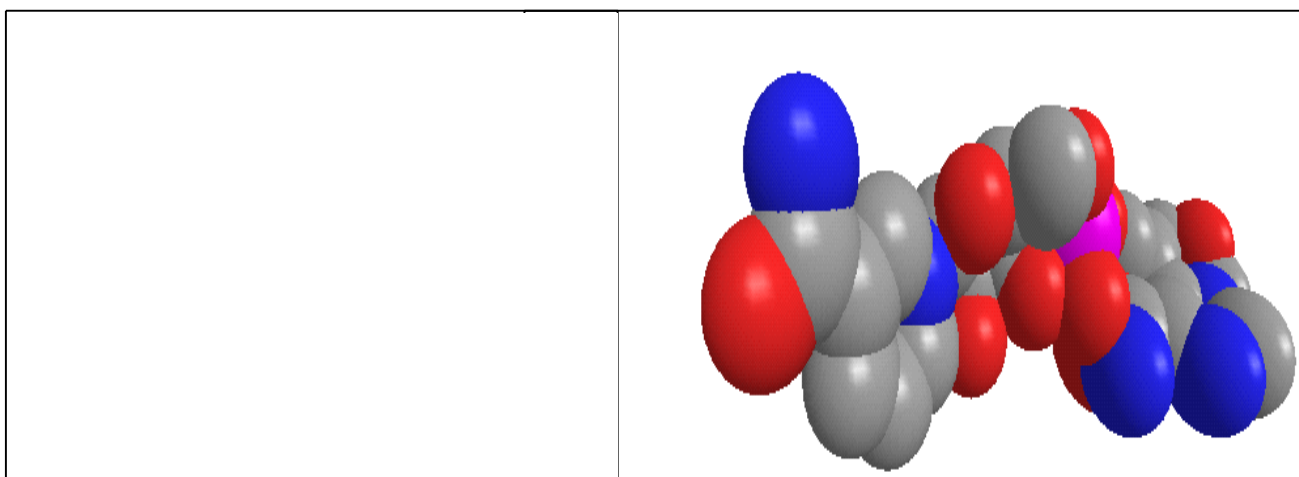
**Scheme 4 Quinonoid- Dihydrobiopterin**

So far, it is suggested that NADH is oxidized to NAD<sup>+</sup> upon transferring a hydride (H<sup>-</sup>) to the N-5 atom of the quinonoid- dihydrobiopterin. To compensate the addition of the hydride to the molecule, another atom must be protonated (Varughese et al., 1994).



**Scheme 5 Proposed mechanism of what happens upon interactions between DHPR and quinonoid-dihydrobiopterin.**

The presence of the NADH in a mixture with the enzyme and the ligand is believed to influence the interactions between the enzyme and its substrate. Consequently, we will also account for the presence of the cofactor in all of the measurements.



**Scheme 6 Structures of NADH, 1, 4-dihyronicotinamide adenine dinucleotide (3D space- filling conformation, left).**

In our study, we primarily use fluorescence spectroscopy to investigate any interactions existing between the enzyme, its cofactor, and its inhibitor. Then, we use infrared spectroscopy to identify characteristic bands in the cofactor's and the inhibitor's structure. We also use computer-generated simulations, using *Ab initio* calculations, to substantiate our experimental infrared data and, later, Raman data.

## II. Protein Extraction and Enzymatic Assay

*Protein extraction* The protein dihydropteridine reductase used in this experiment is obtained from rat liver. The rat liver is purchased and kept at  $-20^{\circ}\text{C}$  until it is ready for use. Before the actual extraction, the liver is thawed at room temperature and cut into small pieces. In this study, approximately 74 g of rat liver are used.

The purification of the protein involves numerous steps. First, in an extraction step, the liver is homogenized in 111 mL 0.03 M cold acetic acid, three times, for 60 seconds each. Then, the mixture is centrifuged for 35 minutes, at 4000xg. The supernatant is then collected and its pH is adjusted to 7.4 using potassium hydroxide. After reaching the targeted pH, the solution is further centrifuged, but this time for ten minutes at 10,000xg.

The second step of the purification is an alkaline ammonium sulfate fractionation, where 78.75 g of the  $(\text{NH}_4)_2\text{SO}_4$  is added to the supernatant from the previous step over a period of 30 minutes (35g of  $(\text{NH}_4)_2\text{SO}_4$  is needed for every 100 mL of supernatant collected). This step is performed on ice, the mixture being stirred. After all the  $(\text{NH}_4)_2\text{SO}_4$  is added, the mixture is left stirring for an additional half- hour. The mixture is centrifuged once again for ten minutes at 10,000xg.

After the third centrifugation, the supernatant is collected and 22.5 mg of  $(\text{NH}_4)_2\text{SO}_4$  is added to it (10 g of  $(\text{NH}_4)_2\text{SO}_4$  is added for every 100 ml of supernatant collected). The mixture is left to stir for 30 minutes then is centrifuged at 10,000xg for ten minutes. Finally, the precipitate is collected and dissolved in 0.01 M Tris- HCl, pH 7.8; its volume is adjusted by adding 0.2x volume of buffer, x being the final volume of the extract. The mixture is dialyzed in 0.01 M Tris- HCl buffer, pH 7.8, for three hours. Then, the buffer is exchanged and the dialysis continues overnight.

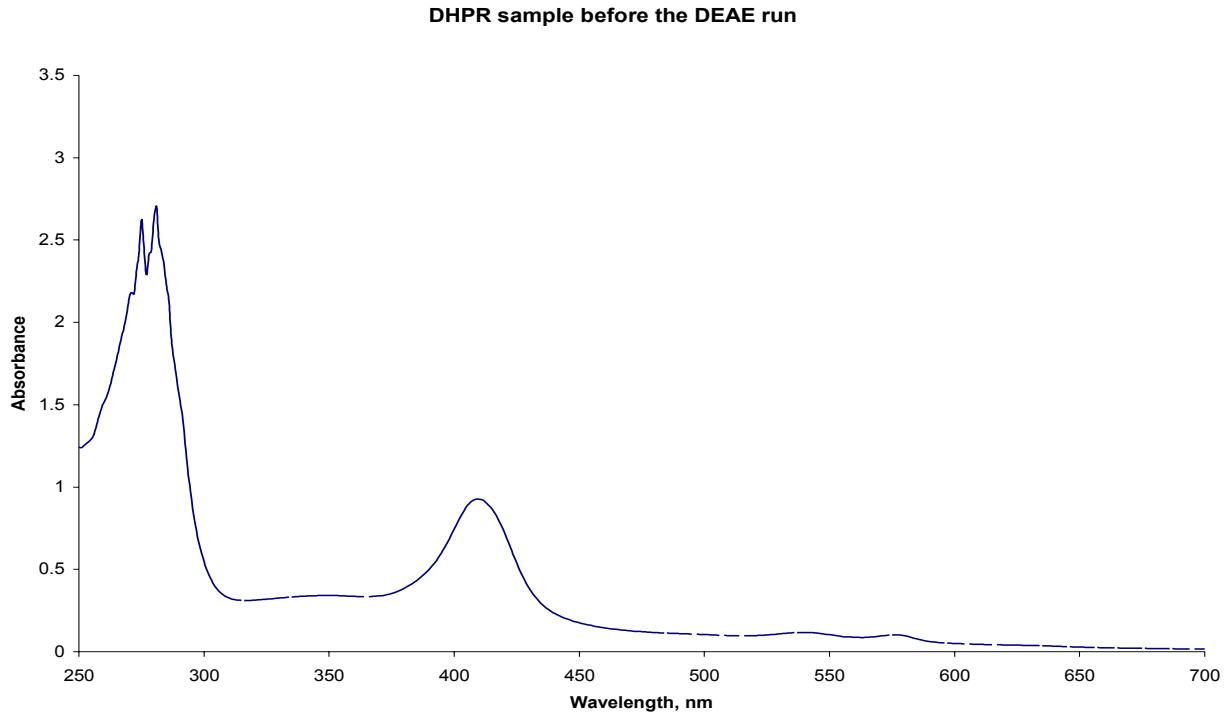


**Figure 1** Absorption spectra of the DHPR after extraction from rat liver.

In the last step of the protein purification, the enzyme is applied to DEAE- cellulose column (2.5 x 35 cm), which is previously equilibrated with 0.01 M Tris- HCl, pH 7.8. The eluate collected is then monitored for enzyme activity (Craine et al., 1972, p. 6984).

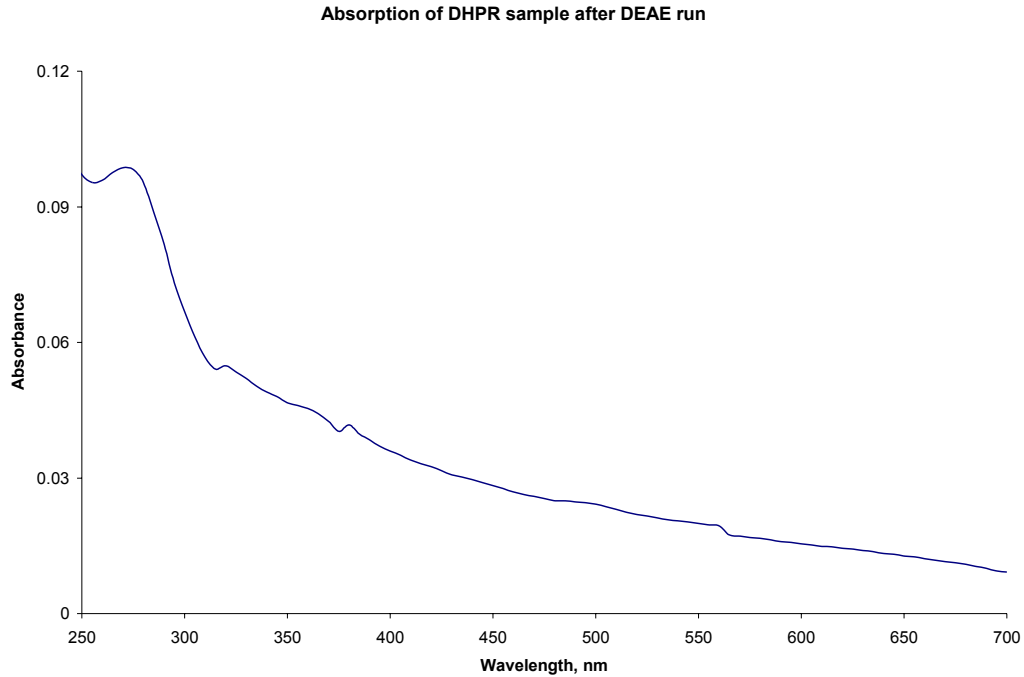
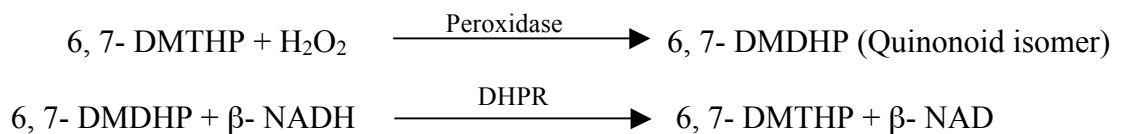


**Figure 2 Absorption spectrum of the DHPR sample collected from DEAE column wash.**

*Enzymatic Assay* After purifying the protein, its activity is verified using a continuous spectrophotometric rate determination method. The method is based on the following chemical reactions:



Five reagents are prepared with respective proportions and mixed to form a test solution and a blank solution. The amounts used are summarized in Table 1 below.

**Table 1** The reagents used to test if the enzyme is viable.

	<b>Reagent</b>	<b>Volume Used (<math>\mu\text{L}</math>)</b>	
		<b>Test</b>	<b>Blank</b>
A	100 mM Tris-HCl Buffer, pH 7.2	750	750
B	0.43 mM $\beta$ - NADH	500	500
C	0.3 % $\text{H}_2\text{O}_2$	15	15
D	2.15 mM 6, 7- DMTHP	25	25
E	Peroxidase	25	25
F	DHPR solution	100	-

The reagents are added in the order A  $\rightarrow$  D  $\rightarrow$  C  $\rightarrow$  E  $\rightarrow$  B  $\rightarrow$  Water  $\rightarrow$  F (135  $\mu\text{L}$  of deionized water is added) and they are mixed by inversion. The activity of DHPR during the reactions is followed via a time driven absorption measurement at 25°C, by monitoring the NADH present (A fixed at  $\lambda_{\text{max, NADH}}$  340 nm). The spectra for the blank and a sample are reported in the following figure (Figure 3).

## Enzymatic Assay of DHPR

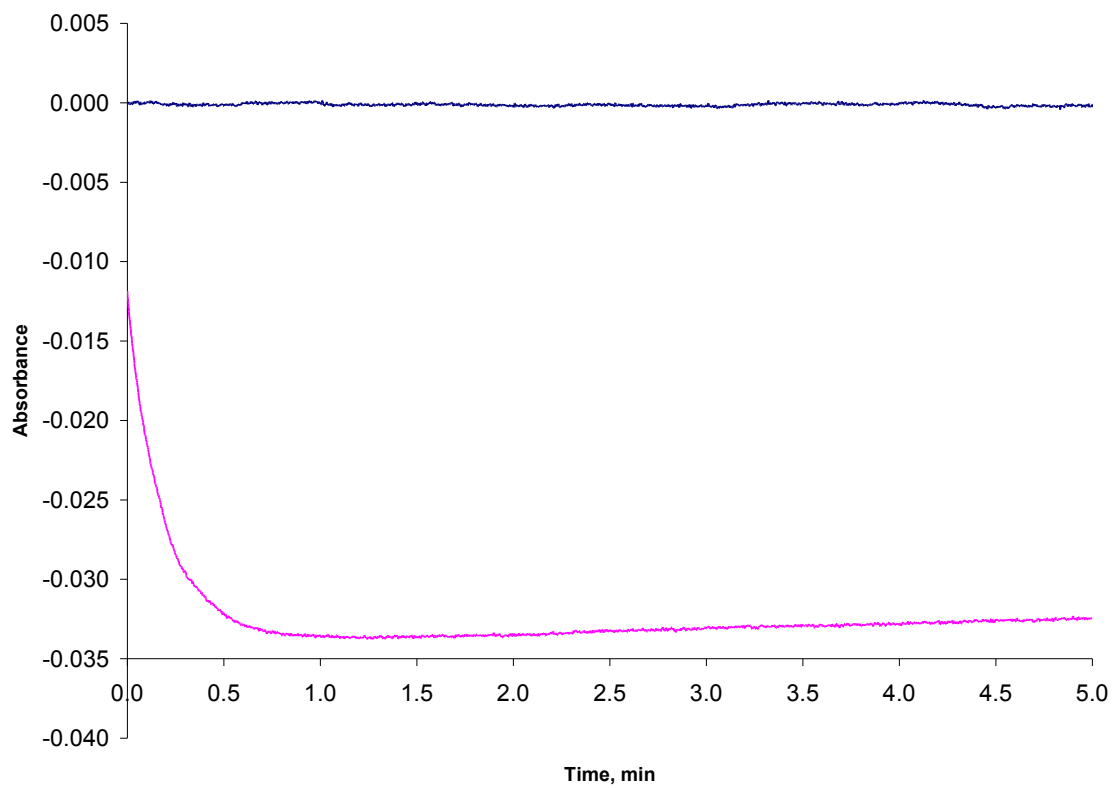
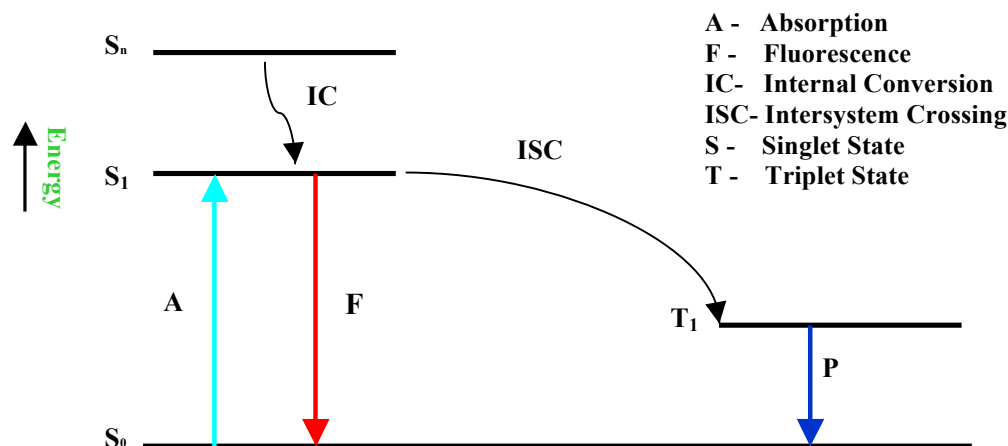


**Figure 3** Quasi- linear absorption spectrum (blue) corresponding to the blank mixture. The bottom graph shows the activity of the DHPR for the first 30 seconds of the reactions (Collected by Karim Walters, 3/23/07).

### III. Methods and Instrumentation

For the absorption and fluorescence measurements, the samples are prepared in 0.05 M Tris- HCl buffer, pH= 7.5, in water. However, for the infrared measurements, the samples are prepared in Tris- HCL buffer in deuterium oxide, of same concentration and pH.

Furthermore, spectroscopy allows the study of the photochemical processes that particles, namely an electron in a given molecule, can undergo. These different processes are summarized in a diagram known as the Jablonski diagram.



Scheme 7 Simplified version of the Jablonski diagram showing the principal photochemical processes.

#### 1. UltraViolet-Visible (UV- Vis) Spectroscopy

The ultraviolet (UV) and the visible (VIS) regions are the portion of the electromagnetic spectrum ranging from 190 nm to 800 nm (Pavia et al., 2001, p. 531). Most organic compounds and their functional groups cannot be detected in that range of wavelength. However, UV-VIS spectroscopy is widely used to complement data obtained from other types of compounds' analysis techniques such as infrared (IR) spectroscopy or nuclear magnetic resonance (NMR) spectroscopy. When a sample is hit by a radiation in UV-VIS measurement, part of the energy of the radiation is absorbed by the sample. The residual radiation then passes through a prism that

produces a spectrum. This spectrum is known as the absorption spectrum. During absorption, an electron of the sample located at a lower energy level is excited to a higher energy level. The instrument used in this study is a double- beam spectrophotometer. The advantage of using a double-beam spectrophotometer resides in the fact that the instrument is set up in such a way that the procedure allows for correction of light intensity variations and detector response with time and wavelength.



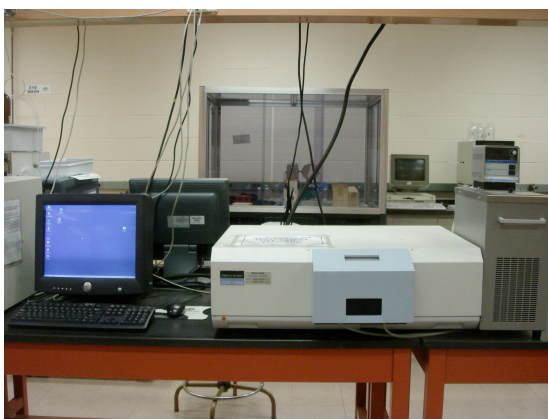
**Scheme 8 Perkin- Elmer Lambda 25 UV-Vis spectrophotometer used in the experiment**

## 2. Fluorescence Spectroscopy

When we hit a molecule with an incident radiation, the amount of the radiation energy it absorbs pulls its electrons to a level of higher energy. However, the electron, being more stable in the lowest energy level, tends to fall back to its initial state. By going back to the lowest energy level, the electron emits radiant energy that we can detect using Fluorescence spectroscopy. Most of the fluorescence techniques allow us to select both the absorbed and the

emitted wavelength. The molecule in its lowest energy level is called a ground state singlet molecule,  $S_0$ , which is subdivided into vibrational states. When this molecule absorbs light and get excited, it can move to higher energy levels known as  $S_1$ . As mentioned previously, the excited molecule does not remain in the excited state and, eventually, it falls back to the ground state. Different processes characterize how the excited molecule returns to its ground state. If the electron falls from the  $S_1$  level to the highest vibrational state of  $S_0$ , the process is known as Internal Conversion (IC). When the electron goes from a  $S_n$  energy level to T energy level, the process is called an Intersystem Crossing (ISC). The transition from the T energy level to the ground state is called Phosphorescence. The transition from  $S_1$  to the ground state ( $S_0$ ) is what is known as fluorescence.

The types of transitions observed in fluorescence are basically the  $\sigma^* \rightarrow \sigma$  transitions, rarely used, and either the  $n \rightarrow \pi^*$  or  $\pi \rightarrow \pi^*$  transitions. During the acquisition of the emission intensity of a sample, the excitation monochromator is set at a fixed wavelength, which corresponds to the wavelength of its maximum absorption peak. For the excitation intensity measurement, the emission monochromator is set at the wavelength of its maximum emission peak.

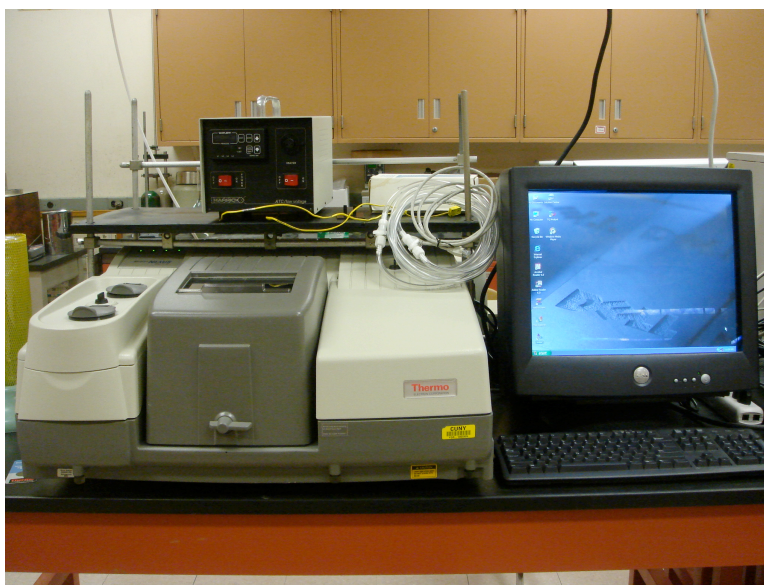


**Scheme 9 Perkin Elmer LS- 50B Fluorescence Spectrophotometer used in this study.**

### 3. Fourier- Transform Infrared (FTIR) Spectroscopy

An important characteristic in a molecule's reactivity is its principal functional groups. Indeed, the functional groups present in a molecule allow one to make suggestions on or determine how that molecule is interacting with other molecules. One technique is usually used to identify the different functional groups of a molecule and this tool is known as Infrared spectroscopy.

Infrared is the region of the electromagnetic spectrum with wavelengths longer than that of the visible light but shorter than microwaves wavelength. Thus, the infrared portion range is from 400 nm to 800 nm (Pavia et al., 2001, p.13). When an infrared radiation hits a sample with a given frequency and the vibrational frequency of the molecules of that sample is similar to that of the radiation, the molecules will absorb some energy. However, not all the bonds in the molecules will absorb the infrared energy. Only the bonds having a dipole moment varying with time will be absorbing the infrared energy. In our experiment, we use Fourier- Transform Infrared spectroscopy (FTIR).



**Scheme 10 Nicolet Nexus 670 FT- IR spectrophotometer used in the experiment.**

#### 4. Ab initio Calculations

To substantiate the data collected experimentally, we perform *Ab initio* calculations for the Trimethoprim and NADH molecule using the calculation softwares GaussView and Gaussian03W. The *Ab initio* methods are described as “methods characterized by the introduction of an arbitrary basis set for expanding the molecular orbitals and then the explicit calculation of all required integrals involving this basis set” (HyperChem Software, Help section).

**Table 2 Summary of the parameters used in the *ab initio* calculations for trimethoprim. The “Raman” option refers to the frequency. With that setting, the software will perform both Infrared and Raman measurements.**

Calculations Set- Up	
<b>Method</b>	DFT/3bLYP
<u>Job Type</u>	Frequency and Optimization
<u>Raman</u>	yes
<u>Basis Set</u>	6- 31G (d)
<u>Charge</u>	0
<u>Spin</u>	Singlet

## IV. Results

### 1. UV- Vis and Fluorescence Spectroscopy

The UV- Vis measurements yield the wavelength at which the fluorescence measurements will be taken. The absorption spectrum for TMP is obtained and its maximum absorbance wavelength is found to be 274 nm. To obtain the emission spectrum of TMP the monochromator for excitation of the spectrophotometer will be fixed at 274 nm. Then, the maximum emission wavelength of TMP will be used to collect its excitation spectrum by fixing the emission monochromator at that maximum wavelength. The excitation and absorption spectra of a given sample overlap and they are both mirror- images of the emission spectrum (cf. Figure 4). The noise level of the absorption spectrum is less than that of the fluorescence spectra because the samples were of different concentrations.

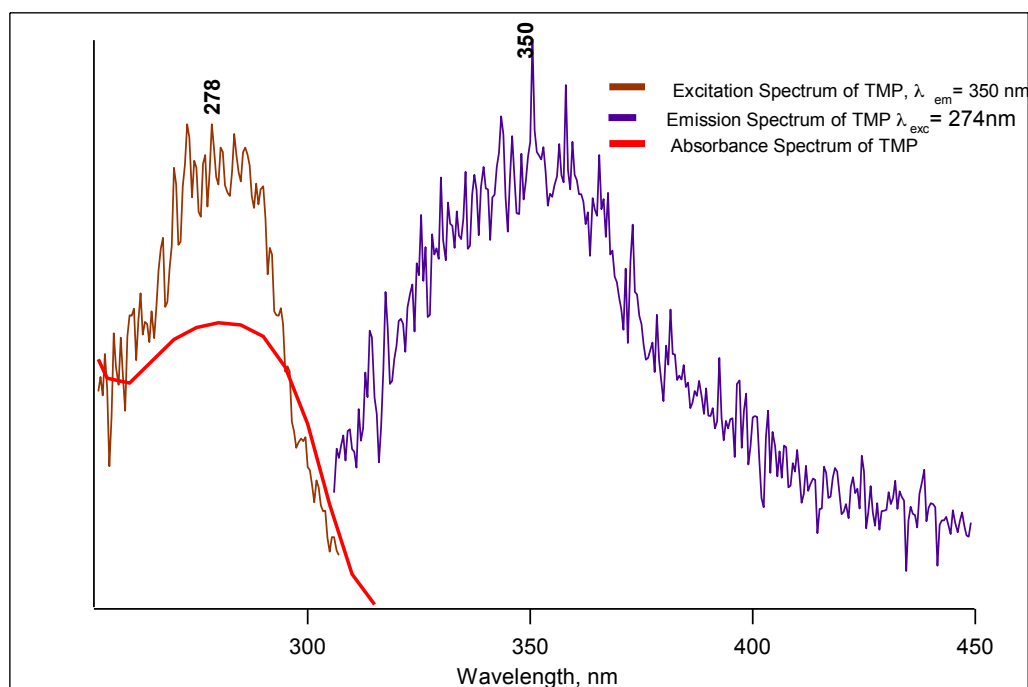


**Figure 4 Absorption (red) and Fluorescence spectra of TMP (emission spectrum in purple, and excitation in brown).**

The spectral characteristics of the enzyme, the ligand, TMP, and of the cofactor, NADH, are first determined individually. Then, mixtures are prepared to study their behavior when they are in presence of each other. Binary mixtures are prepared containing both DHPR and TMP, or containing DHPR and NADH. Ternary mixture refers to solution containing DHPR, TMP and NADH.

The Fluorescence measurements for the mixtures are taken at wavelengths corresponding to the maximum wavelength of each of the moieties under study. Thus, the emission measurements are taken at 274, 280 and 340 nm, which correspond to the absorption  $\lambda_{\max}$  of TMP, DHPR, and NADH, respectively. The excitation spectra are collected at 350 and 450 nm, the emission  $\lambda_{\max}$  of TMP, DHPR, and NADH, respectively.

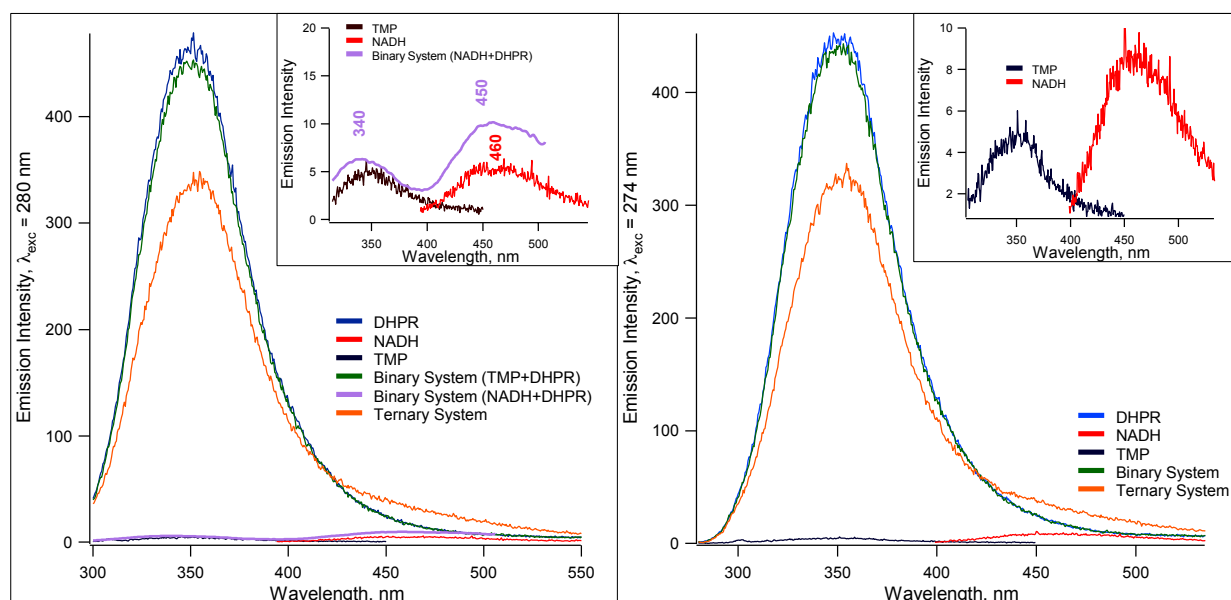


**Figure 5** Emission measurements where the protein is excited (left) and where the TMP is excited (right).

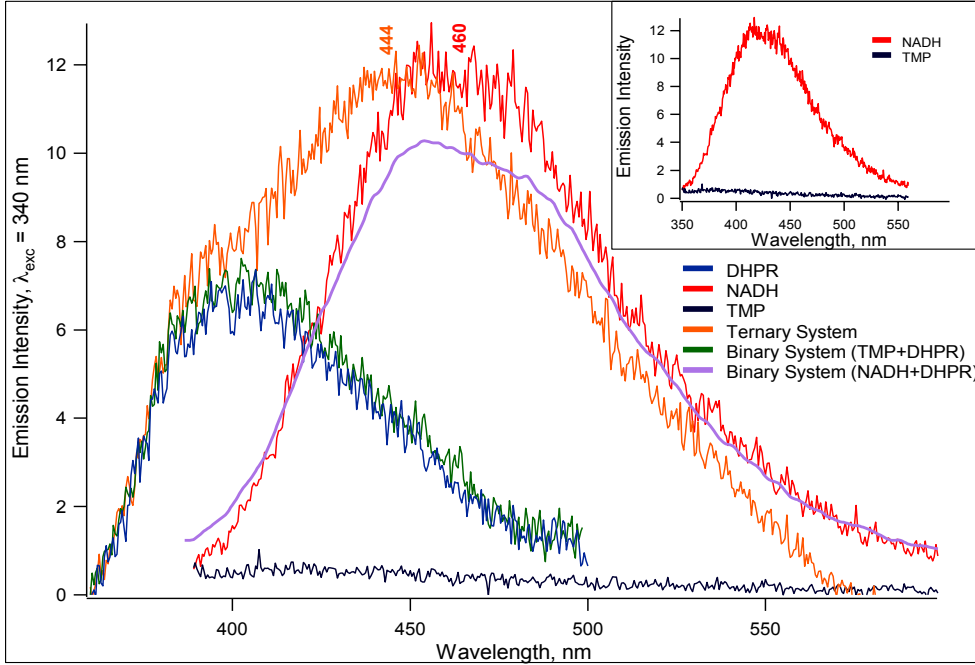


Figure 6 Emission spectra of the samples when excited at the NADH's maximum absorption wavelength.

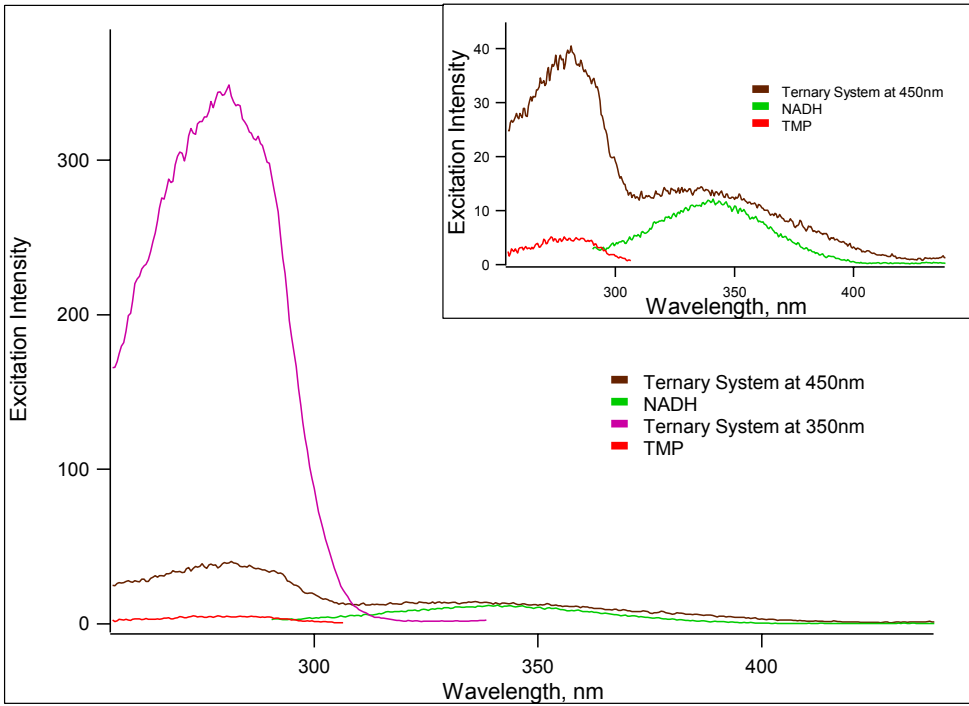


Figure 7 Excitation spectra collected for some samples.

Obtaining the excitation spectra for a given sample allows one to verify the presence of the moieties in the mixtures. Basically, the ternary mixture is excited both at the emission  $\lambda_{\max}$  of TMP and NADH. Figure 7 shows that both TMP and NADH are indeed present in the ternary mixture.

## 2. Infrared Spectroscopy and Calculations- generated Data

Figure 8 shows the infrared spectra obtained for 10.4 mM TMP and NADH solutions prepared in Tris- HCl in D<sub>2</sub>O buffer, pH 7.5.

The infrared spectrum of NADH shows various peaks in the 1550- 1640 cm<sup>-1</sup> region where bending occurs for primary amines. Medium to strong absorption in the 1450- 1600 cm<sup>-1</sup> region often corresponds to aromatic ring vibrations. Also, ring stretch absorption usually appears at 1475 and 1600 cm<sup>-1</sup>. Finally, the region extending from 1600 to 1660 cm<sup>-1</sup> corresponds to stretching vibrations for C=C bonds (Pavia et al., 2001, p. 24- 74).

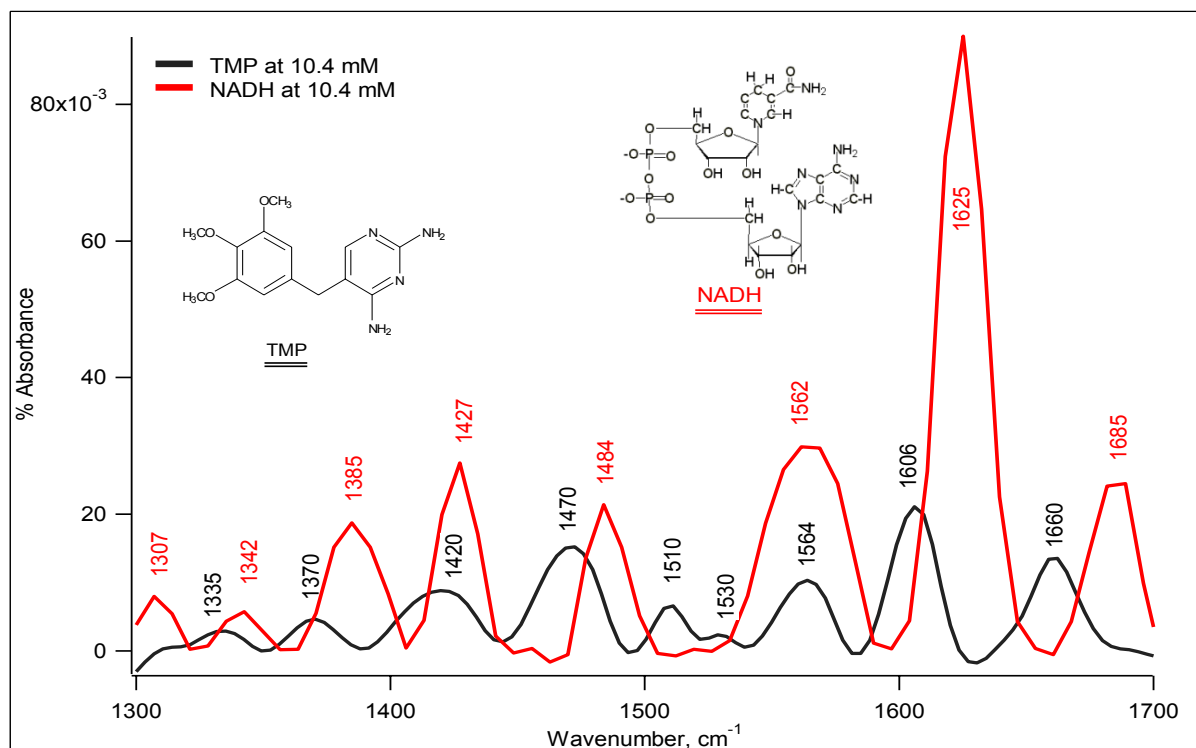


**Figure 8** Infrared spectra for TMP and NADH, indicating their characteristics frequencies.

In addition to the measured infrared spectra of the samples, a simulated infrared spectrum for TMP is obtained using Gaussian calculations software. This spectrum is compared to the experimental spectrum to validate the peaks observed as being real peaks. The simulated spectrum is shown in Figure 9 with the optimized structure of the TMP, also generated by the software.

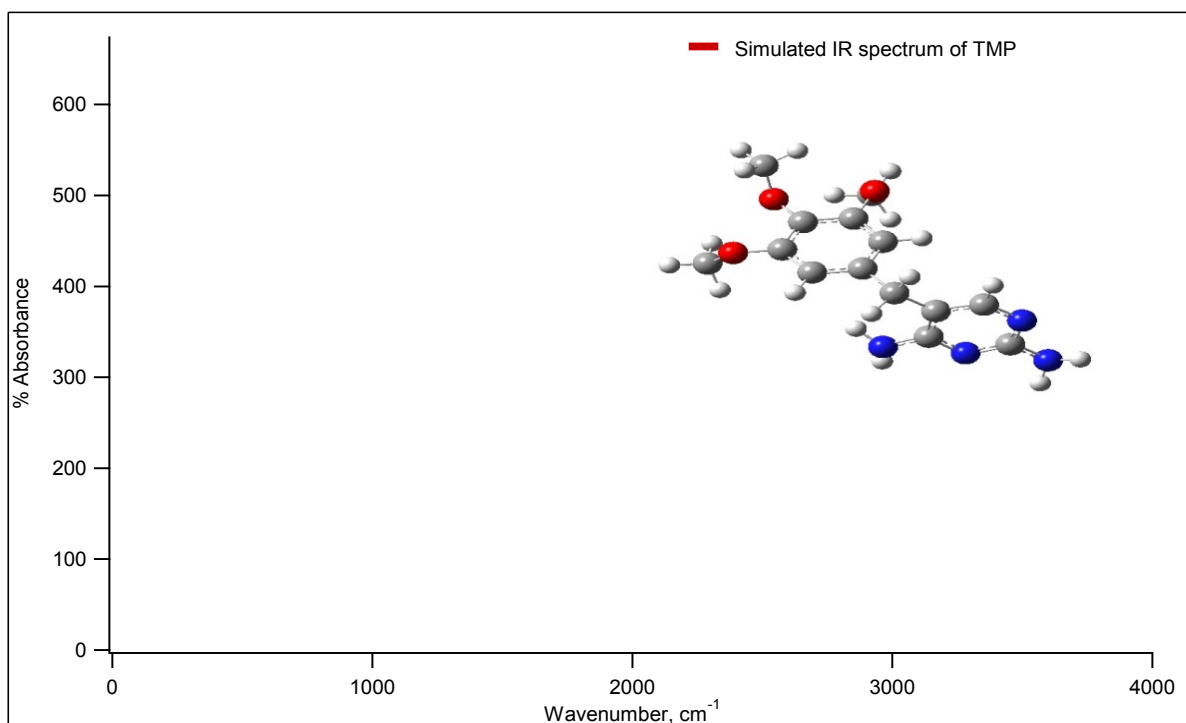


**Figure 9 Simulated Infrared spectrum and optimized structure of the TMP molecule.**

The frequencies observed in the simulated infrared spectrum correspond to the vibration of different parts of the molecule. The displacements occurring in the region of interest are shown in the following figure. The displacement vectors indicate the functional group that might be involved in the binding process.

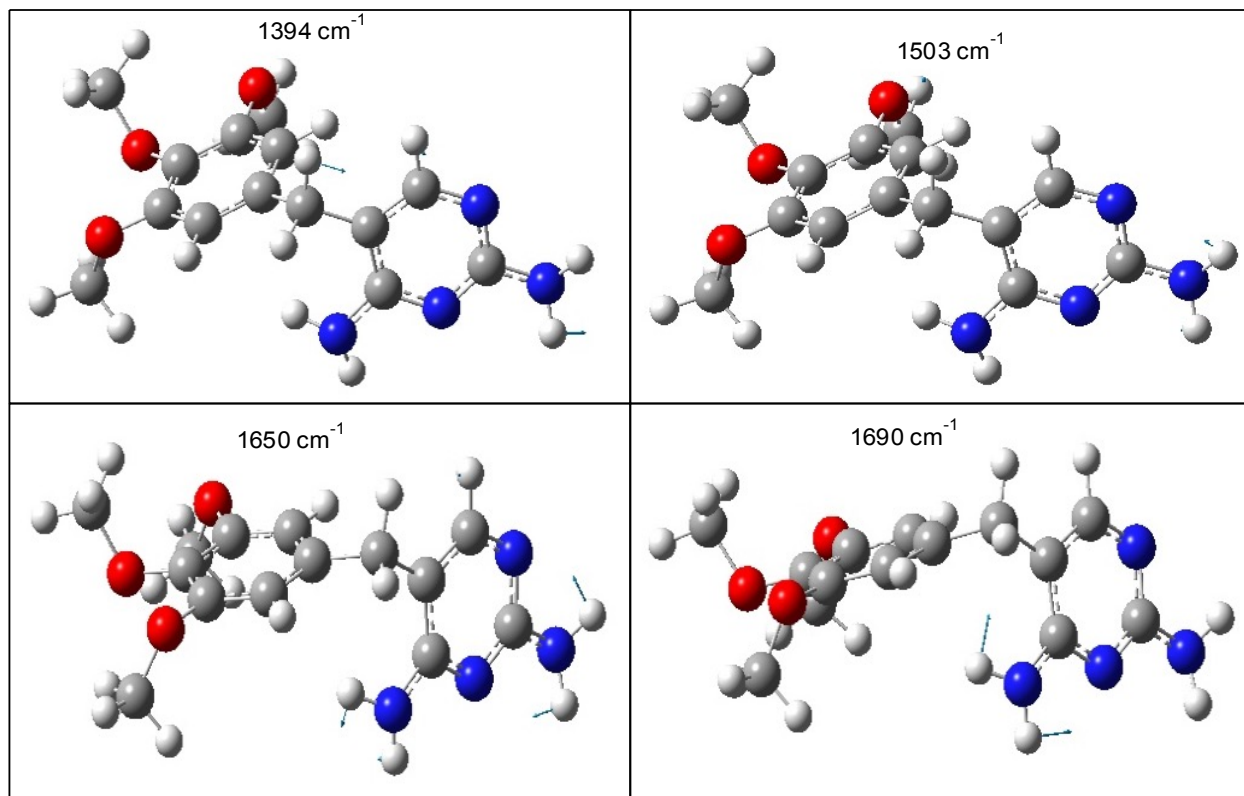


**Figure 10** Displacement, shown with arrows, of characteristic frequency peaks of the TMP molecule.

The simulated infrared spectrum of TMP is superimposed to its measured infrared spectrum in Figure 11. In general, a similar pattern is observed. The two spectra are not exactly identical because the conditions imposed on the molecule are different. In the calculations, the molecule is considered to be in a vacuum, whereas in the experiment, the molecule was in solution.

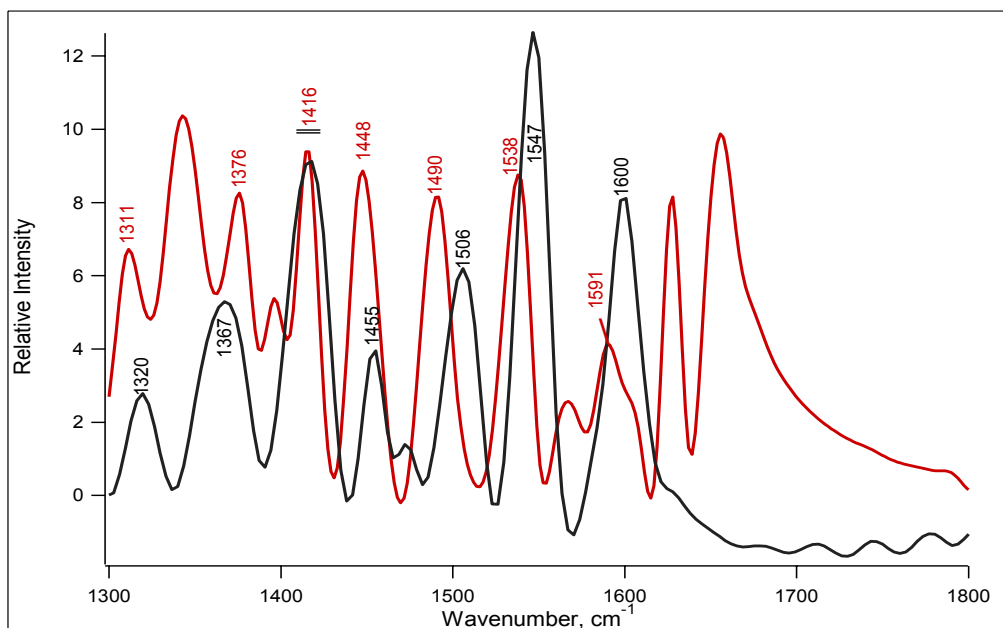


**Figure 11 Comparison of the infrared spectrum of TMP generated by the calculations and that obtained for the actual sample.**

Both in the simulated infrared spectra of TMP and in the experimental infrared spectrum collected, most of the absorption modes appear in the 1450- 1600  $\text{cm}^{-1}$  range, which corresponds to stretching absorption of aromatic rings. In addition, the 1455  $\text{cm}^{-1}$  peak in the experimental spectrum TMP and the 1375  $\text{cm}^{-1}$  peak in the simulated infrared spectrum of TMP are both due to hydrocarbons' vibration modes (Pavia et al., 2001, p. 24- 74).

As the purpose of this study is to understand the mechanism of DHPR's activity by determining what happens upon reaction with its substrate, the TMP molecule is modified and its infrared spectrum also generated using the Gaussian software. The data thus collected mimic what one should observe when the infrared spectrum of the mixture of DHPR and TMP is obtained. The simulated infrared spectrum of the modified TMP molecule is shown in Figure 12.

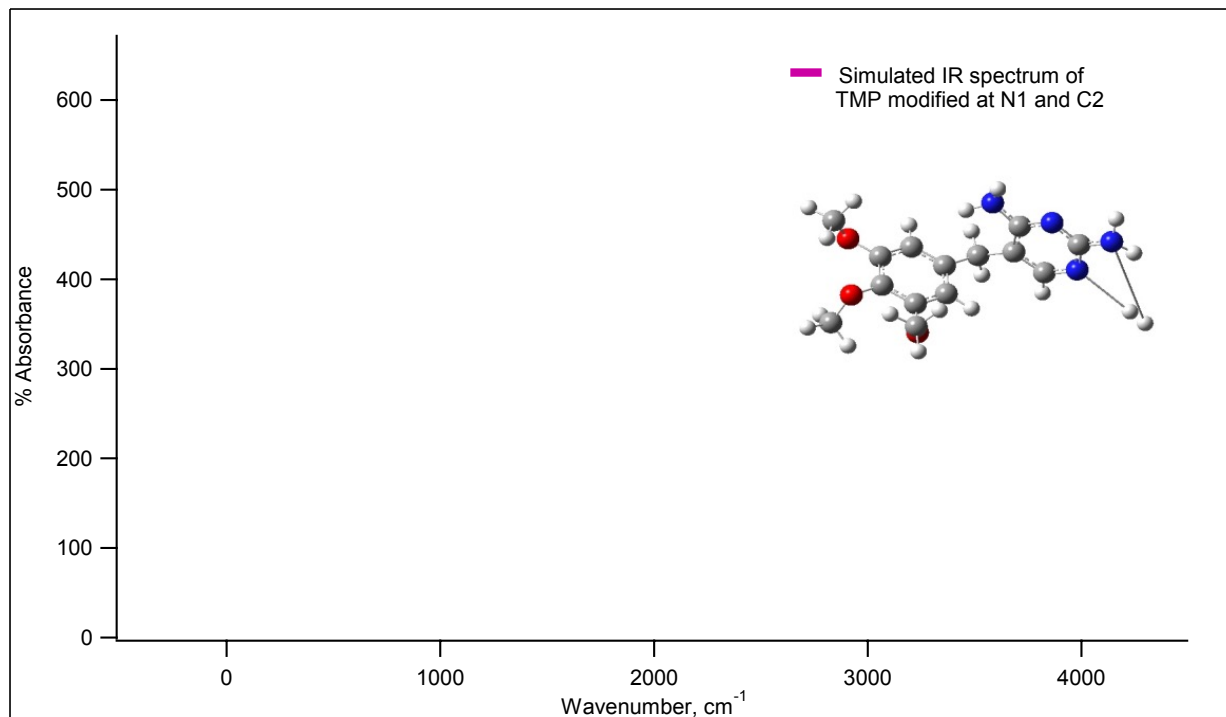


**Figure 12 Simulated infrared spectrum of the modified TMP molecule: a hydride (H) was added to the nitrogen atom at position 1(N-1) and the NH<sub>2</sub> group on the carbon at position 2 (C-2) was protonated.**

The simulated spectrum of the modified TMP also yields characteristic frequency peaks, which are presented in Figure 13. We notice that the protons added to the molecule are pushed away during the calculations, which suggests that the molecule does not handle the +2 charge imposed on it. That might be why the proposed mechanism suggested that only one proton be added at a time.

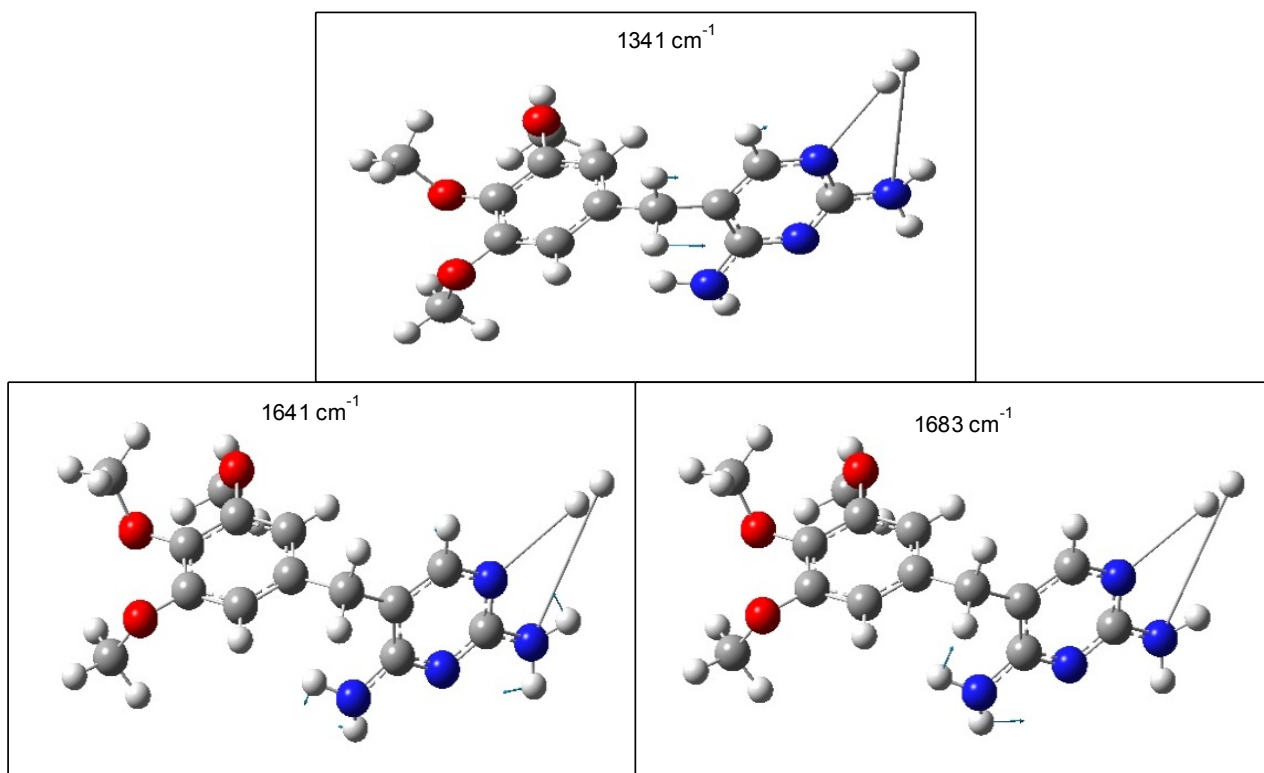


**Figure 13 Displacement of the vibration modes characteristic to the TMP molecule modified at N-1 and at the  $\text{NH}_2$  group attached to C-2.**

The comparison of the simulated infrared spectra of normal TMP and that of the modified TMP allows us to identify the vibration modes that vary or do not change upon modifications. Those vibration modes can be used as biomarkers to indicate which functional groups of the TMP molecule are actively involved in the reaction process. For example, the 1394 and 1469  $\text{cm}^{-1}$  peaks for the normal TMP shift to 1411 and 1479  $\text{cm}^{-1}$  in the modified TMP, respectively, while the 1429 and 1547  $\text{cm}^{-1}$  peaks remain the same in both spectra. The respective simulated spectra are put together in Figure 14 to allow for a better comparison of the two.

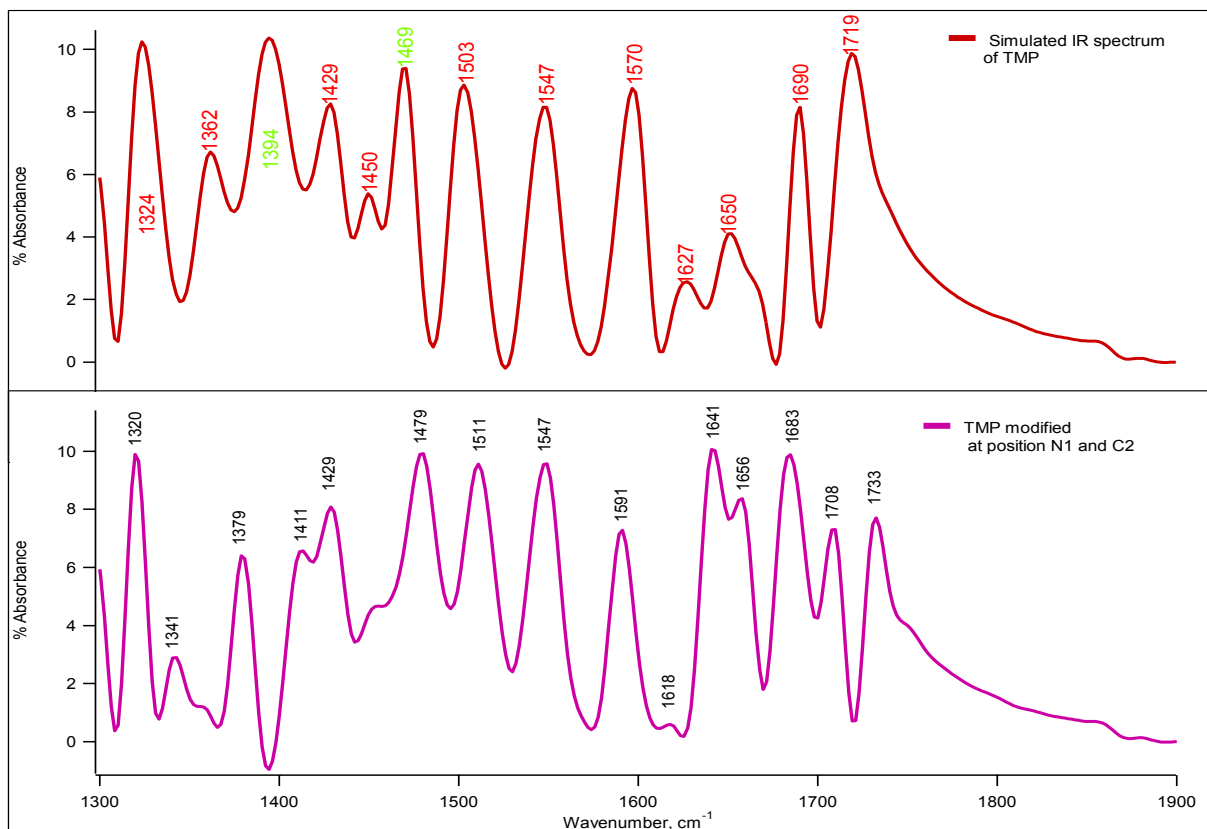


Figure 14 Comparison of the simulated infrared spectra for the TMP molecule (top) and the modified TMP molecule (bottom).

## V. Discussion and Conclusion

*Fluorescence Measurements* Once we collect and process our data for the individual molecules and their binary and ternary mixtures, we compare the spectra obtained when we excite the samples at the enzyme's maximum absorption peak and at that of TMP. We observe that, for a same concentration of DHPR, there is not a significant variation in the emission intensity of the protein in the binary mixture with TMP, suggesting that the interactions between the two are negligible if not nonexistent. In the ternary mixture, the emission intensity of the protein decreases significantly with the addition of the cofactor, NADH. This means that NADH is very important in enhancing the interactions between the enzyme and its ligand, TMP. Such findings agree with the observations made in other research projects that NADH helps with the stability of the enzyme and make its active site more available to its ligands (Su et al., 1993, 1994; Varughese et al., 1992). Similar observations are made when the samples are excited at the TMP's characteristic wavelength. The emission intensity for the Trimethoprim by itself is lower than its emission intensity in the binary mixture and in the ternary mixture. Based on such observations, we conclude that TMP, being in a mixture, may be getting some energy from the other component(s), which would explain the increase in its emission intensity. Yet, how do we confirm the presence of the component in the mixtures?

To answer the above question, we proceed to obtain the excitation spectra of the ternary mixture excited at wavelengths within the maximum emission peak of TMP and NADH respectively, and we compare them to the excitation spectra of TMP and NADH. We see that, when we excite the ternary mixture at the TMP maximum emission wavelength, the peak for the ternary mixture overlays that of the TMP's excitation peak. Similarly, when the ternary mixture is excited at the NADH maximum emission wavelength, the peak observed also overlaps the

NADH's excitation peak. Thus, the data confirm that the ternary mixture actually contains the ligand and the cofactor. From the data obtained in the fluorescence measurements, it is concluded that the samples being studied are interacting with each other.

*Infrared Spectroscopy and Simulations* After determining that there are interactions between the molecules, one needs to figure out the exact nature of these interactions. This is done with the infrared measurements, which can specify the characteristic vibration modes of the molecules. The infrared spectra reported only show the 1300- 2000  $\text{cm}^{-1}$  region, which is believed to be the area with the most characteristic peaks for the molecules.

From the *Ab initio* calculations, we were able to obtain Infrared spectrum for both the normal trimethoprim molecule and its modified form. From those spectra, we identified vibrational frequencies that can be used as markers. Basically, we can use the frequency modes corresponding to the atoms believed to be involved in the binding process, modify their environment and observe how the Infrared spectrum is affected. Then, we could compare the spectrum obtained for the ligand by itself the spectra we will obtain for the binary and ternary mixtures. We could also monitor which functional groups of the ligand are involved in binding the enzyme.

Also, the calculations give some insight on the structure of the trimethoprim molecule, in which the presence of two rings would suggest a planar structure. The optimized structure generated (cf. Figure 9) shows that these two rings are not co-planar, but instead they are at a certain angle of each other.

Later, we will obtain the infrared measurements for the binary and ternary mixtures. Then, we will run Raman spectroscopy for our samples to complement the data obtained from the Infrared spectroscopy. We will also run transient fluorescence measurements to get information on the kinetics of the reactions happening between the enzyme and its ligands.

## **Acknowledgements**

I thank the McNair Scholar Program, UNCF/Merck Science Initiative, the Louis Stokes Alliance for Minority Participation in Sciences, Mathematics and Engineering, the York Honors Program and PSC-CUNY for supporting my undergraduate research training. I specially thank my mentor Dr. Ruel Z.B. Desamero for helping me find the best in me and for his tireless assistance. I also thank my lab collaborators, Justina Chinwong, Chrystal Dol, Tharenie Sivarajah, Janie Quizhpi, and Karim Walters, and anyone whose actions make my research training possible.

## References

- Craine, J. et al. (1972). The isolation and characterization of dihydropteridine reductase from sheep liver. *The Journal of Biological Chemistry*, 247 (19), 6082- 6091. Retrieved October, 16 2006 from [www.jbc.org](http://www.jbc.org).
- Kaufman, S., et al. (1975). Phenylketonuria due to a deficiency of dihydropteridine reductase. *New England Journal of Medicine*, 293, 785- 790.
- Nylan, W. L. (1984). Fifty years ago: Asbjörn Fölling and phenylketonuria. *Trends Biochem. Sci.*, 9, 71-72.
- Pavia, D., Kriz, G., & Lampman, G. (2001). *Introduction to spectroscopy: A guide for students of organic chemistry* (3rd ed.). Washington: Brooks/ Cole Thomson Learning, 13, 24-74, 531.
- Schuet, V. (2001). *Brain Phe and PKU: Summary of a presentation by Dr. Richard Koch, Los Angeles Children's Hospital*. Retrieved from [www.pkunews.org/research/koch.htm](http://www.pkunews.org/research/koch.htm), March 23rd 2007.
- Su, Y et al. (1993). The crystallographic structure of a human dihydropteridine reductase NADH binary complex expressed in Escherichia coli by a cDNA constructed from its rat homologue. *J. Biol Chem.* ,268, 26836- 26841.
- Su, Y. et al. (1994). Crystal structure of a monoclinic form of dihydropteridine reductase from rat liver. *Acta Cryst. D50*, 884- 888.
- Varughese, K. et al. (1992). Crystal structure of rat liver dihydropteridine reductase. *Proc. Natl. Acad. Sci. USA* , 89, 6080- 6084.

Varughese, K. et al. (1994). Structural and mechanistic characteristics of dihydropteridine reductase: A member of the Tyr- (Xaa)<sub>3</sub>- Lys- containing family of reductases and dehydrogenases. *Proc. Natl. Acad. Sci. USA*, 91, 5582- 5586.

Webber, S. et al. (1978). The purification of rat and sheep liver dihydropteridine reductases by affinity chromatography on methotrexate-sepharose. *Analytical Biochemistry*, 84 (2), 491-503. Cited in “Enzymatic Assay of Dihydropteridine Reductase” from [www.sigmaaldrich.com](http://www.sigmaaldrich.com).

\*\*\*\*\*